ACCEPTED ARTICLE

Classification of some Iranian *Vicia* species using SEM image analysis coupled with conventional texture analysis and deep learning

Mehrnoosh Jafari[1*], Seyed Ali Mohammad Mirmohammady Maibody[2], and Mohammad Hossein Ehtemam[2]

1. Department of Biosystems Engineering, College of Agriculture, Isfahan University of Technology, Isfahan 84156-83111, Islamic Republic of Iran.
*Corresponding Author; e-mail: m.jafari@iut.ac.ir
2. Department of Agronomy and Plant Breeding, College of Agriculture, Isfahan University of Technology, Isfahan 84156-83111, Islamic Republic of Iran.

Abstract

Micromorphological characteristics of seed sculpturing might be effective in circumscribing the infra-specific taxa in the genus *Vicia*. The present study was conducted to determine whether microstructural and seed coat texture data obtained from SEM images can serve as sufficient tools for delimiting *Vicia* genus. Other than visual inspections, a variety of texture-based methods, including the four conventional approaches of GLCM, LBP, LBGLCM, and SFTA, and the four pre-trained convolutional neural networks (namely. ResNet50, VGG16, VGG19, and Xception models) were employed to extract features and to classify the species of *Vicia* genus using SEM images. In a subsequent step, the four unsupervised k-means, Mean-shift, agglomerative, and Gaussian mixture classification methods were exploited to group the identified *Vicia* spices based on the underlying features thus extracted. Moreover, the three supervised classifiers of multilayer perceptron network (MLP), Support Vector Machine (SVM), and k-nearest neighbor (kNN) were compared in terms of capability in discriminating the different visually-identified classes. SEM results showed that three classes might be identified based on the micromorphological character-species connections and that the differences among the species in the *Vicia* genus and the validity of *Vicia sativa* could be confirmed. Regarding the performance of the classifiers, SFTA textural descriptor outperformed the GLCM, LBP and LBGLCM algorithms but yielded a decreased accuracy compared with deep learning models. The combined Xception model and a MLP classifier was successful to discriminate the species in the *Vicia* genus with the best classification performances of 99% and 96% in training and testing, respectively.

Keywords: Scanning electron microscope (SEM), seed sculpturing, *Vicia*, micromorphology, plant taxonomy, Convolutional neural networks.

1. Introduction

Taxonomy identification methods involve destructive sampling followed by physical, physiological, biochemical, and molecular determinations (Luo et al. 2021). Scanning electron microscopy (SEM) and light microscopy (LM) have recently been used as important non-destructive taxonomic delimitation tools for various families and genera (Ilakiya and Ramamoorthy 2021; Jalal et al. 2021). SEM analysis of the seed coat surface has revealed genetic diversity among *Astragaleae* and *Trifolieae* (Rashid et al. 2021), *Vicieae* (Rashid et al. 2018), *Geranium* (Aedo 2016), Brassicaceae (Gabr 2018), *Hypericum* (Szkudlarz and Celka 2016), and so on. More recently, visual assessment of SEM images has been coupled with computer-aided image processing for better interpretation of SEM images to attain precise and automatic identification of genera.

Seed surface ornamentation may be a useful and rich source of data for clustering or classification based on feature determination. SEM coupled with image analysis offers a powerful tool for evaluating microstructural changes (Pieniazek and Messina 2016). However, the question remains whether species delimitation and identification can be solely based on microstructural data and seed coat texture traits.

From among the few detailed studies reported on seed species identification using SEM coupled with image analysis, one is Prasad *et al.* in which an image processing software was used to analyze the seed coat structure of 23 cultivated and six wild sesame germplasms obtained from digital and SEM images (Prasad et al. 2014). The results indicated that the seeds of wild sesame species could be well differentiated from those of the cultivated varieties based on shape and architectural analyses. Pieniazek and Messina conducted SEM image analysis as an alternative to the analysis of the effects of freeze-drying on the microstructure and texture of legume and vegetables (Pieniazek and Messina 2016). Results revealed the success of the combined SEM and classical texture analysis methods as a useful tool for the investigation of quality parameters.

Depending on the method used for extracting textural features, classical texture analysis techniques can be quite diverse and varied (Ribas et al. 2020). In recent years, new methods based on transfer learning with deep convolutional neural networks (CNNs) have emerged that outperform the classical texture analysis in terms of the significantly better results they yield (Liu X and Aldrich 2022).

CNNs used to classify seeds have been extensively reported on in the literature in order to illustrate their applications in recognizing an individual barley kernel variety with satisfactory accuracy (Kozłowski et al. 2019), determining the viability of mechanically scarified *Quercus* *robur* L. seeds (Przybyło and Jabłoński 2019), identifying Chickpea (*Cicer arietinum* L.) seed varieties (Taheri-Garavand et al. 2021), assessing seed germination in three different crops (namely, *Zea mays*, *Secale cereale*, and *Pennisetum glaucum*) (Genze et al. 2020), and obtaining high-throughput soybean seed phenotypes with efficient calculation of morphological parameters (Yang et al. 2021). So far, the application of CNNs in classifying varieties based on SEM images of seed coat has been mentioned in only one study, in which five different network architectures were trained for classifying *Allium* seed walls based on recognizing SEM images (Ariunzaya et al. 2023). Nonetheless, no study has yet been reported on the application of CNNs in classifying varieties based on SEM images of seed coat surfaces.

It is the objective of the present work to investigate the potential of seed coat sculpturing in the taxonomy of the genus *Vicia*, describe seed coat sculpturing at a specific level among the Iranian species, and evaluate the diagnostic value of this character in terms of variability among populations of *Vicia*. Moreover, the current study endeavors to examine the architecture of deep learning convolutional neural networks and some classical texture analysis methods with respect to their capabilities in categorizing *Vicia* species.

2. **Materials and Methods**

The methodology used in this work consists of the following five stages: 1) SEM image acquisition, 2) visual observation of the SEM images thus acquired, 3) classical and deep feature extraction, 4) feature dimensionality reduction, and 5) clustering and classification. The block diagram illustrating the image processing and data mining steps involved in the proposed methodology is presented in Figure 1.

2.1 Plant material

For the purposes of this study, ninety seed samples belonging to 18 *Vicia* species were collected mostly from different locations in Iran. Voucher specimens of the wild specimens and those obtained from the herbarium were deposited at the Herbarium Conservation Center of Isfahan University of Technology (Table 1). In order to provide samples with herbarium specimen labels, the accessions were grown in Chah-Anari Research Farm of Isfahan University of Technology.

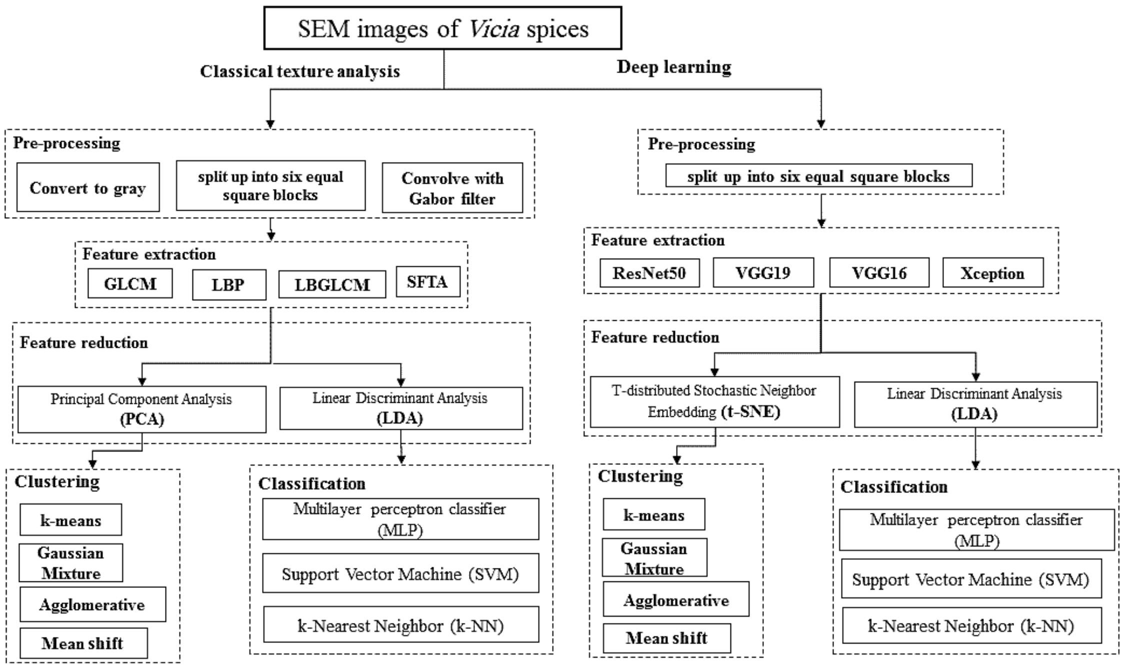

Figure 1. Block diagram of the proposed methodology.

2.2 SEM image acquisition

A minimum number of three mature, clean, and perfect seeds from each accession were used for taking SEM images and the subsequent analyses. The seeds were mounted on a twin-walled conductive metal stand and prepared without any dehydration using a gold grain of approximately 8-30nm thick and a BAL-TEC (Baizers) SCD 005 Sputter Coater. SEM photos from the lateral and frontal views were then taken at different magnifications (SEM, Model XL30, PHILIPS – EDAX). The density of the projections per square mm of the area at a given magnification (9 cm^2 at a magnification of 1000, representing 900 μm) was determined thoroughly on the display screen. Other useful specifications such as projection height, form, number, and ridge sharpness were measured and recorded. Stern (Stern 1983) terminology was used to describe the SEM images.

Table 1. Voucher specimens and herbarium data of the selected species of *Vicia* used in the SEM study of seed micromorphology.

No.	Species/ Section	Herbarium number	Location/Province	Currently herbarium nomenclature
	Sect. Anatropostylia			
1	*V. koeieana*	2510	Bakhtaran	*V. koeieana* Rech. F.
	Sect. Cracca			
2	*V. aucheri*	5698	Mazandaran	*V. aucheri* Boiss.
3	*V. cracca*	99	Isfahan	*Vicia cracca* (L.)
4	*V. akhmaghanica*	3774	West Azarbayegan	*V. akhmaghanica* Kazar
5	*V. cappadocica*	19571	West Azarbayegan	*V. cappadocica* Boiss & Bal.
6	*V.ciceroidea*	12292	Tehran	*V.ciceroidea* Boiss
7	*V. cinerea*	49536	BandarAbbas	*V. monantha* Retz. subsp. *monantha* Retz.
8	*V. crocea*	12781	Gorgan	*V. crocea* (Desf.) B. Fedstch.
9	*V. multijuga*	51707	Tehran	*V. multijuga* (Boiss.) Rech. f.,V.
10	*V. variabilis*	45924	Fars	*V. variabilis* Grossh.
11	*V. villosa*	26316	Lorestan	*V. villosa* Roth
	Sect. Ervilia			
12	*V. ervilia*	63125	Khozestan	*V. ervilia* (L.) Willd
13	*V. tetrasperma*	28867	Islamshar	*V. tetrasperma* (L.) Schreb.
	Sect. Vicia			
14	*V. angustifolia*	60254	Gilan	*V. sativa* subsp. nigra (L.) Ehrh.
15	*V. hyrcanica*	7/4	Isfahan	*V. hyrcanica* Fisch & C. A. Mey.
16	*V. michauxii*	20/2	Isfahan	*V. michauxii* Spreng
17	*V. pregrina*	24/2	Isfahan	*V. pregrina*
18	*V. sativa*	8714	Mazandaran	*V. sativa L.*

2.3 Extracting classical texture features

Classical image texture analysis was carried out using Open CV and Scikit-image libraries of the Python programming language. Texture features were extracted from thirty-six distinctive frontal and lateral SEM images taken at different magnifications from eighteen different *Vicia* species. Image augmentation was used to generate new transformed versions of images to increase the size and diversity of the dataset. The images were initially read and converted to grayscale before they were split up into six equal square blocks. Each block was convolved with Gabor filter, which is an orientation sensitive filter used for texture analysis to achieve the highest response at edges where texture changes (Kaus et al. 2001).

To extract texture features, use was made of four of the successful high-level feature extraction algorithms, including gray level co-occurrence matrix (GLCM), local binary pattern (LBP), local binary gray level co-occurrence matrix (LBGLCM), and segmentation-based fractal texture analysis (SFTA) (Table 2). These texture descriptors were computed and stored for later comparisons.

Table 2 Number of features extracted by the different classical image texture analysis methods.

Classical image texture analysis method	No. of features extracted	Variance ratio (%)			
		PC1	PC2	PC3	Overall
GLCM	20	50.1	32.6	-	82.7
LPB	26	64.32	20.98	-	85.3
LBGLCM	20	70.15	19.98	-	90.13
SFTA	48	36.54	25.64	19.65	81.83

2.4. Feature extraction using pre-trained CNN models

The feasibility of CNN discrimination was investigated in the present work by loading four pre-trained models with pre-trained weights using python Tensorflow and Keras frameworks. The pre-trained convolutional networks used in this study (namely, ResNet50, VGG16, VGG19, and Xception) had been trained on features from ImageNet database and were 50, 16, 19, and 71 layers deep, respectively (Table 3), with network depth defined as the largest number of sequential convolutional or fully-connected layers on a path from the input layer to the output one. The last fully-connected layer of each network was removed, the model weights were frozen, and the networks were used as feature extractors.

Table 3. Specifications of the pre-trained CNNs.

Pretrained CNNs	Network depth	Image size	Non-trainable parameters	No. of output features	No. of PCs to reach 80% variance of the dataset
ResNet50	50	224×224×3	23,587,712	2048	117
VGG16	16	224×224×3	14,714,688	512	117
VGG19	19	224×224×3	20,024,384	512	117
Xception	71	229×229×3	20,861,480	2048	68

2.5 Dimensionality reduction

The dimensionality of the feature space was reduced by Principal Component Analysis (PCA) as an unsupervised dimensionality reduction technique. The number of PCs was selected so as to reach a minimum variance of 80% of the data (Tables 2 and 3). Given the large number of principal components, the data were visualized using the t-SNE dimensionality reduction method for better performance of the deep feature extractors.

2.5 Clustering and classification

The conventional and deep feature sets were used as input to the centroid-based (i.e., k-means), density-based (i.e., mean shift), probabilistic (i.e., Gaussian mixture), and hierarchical (i.e., agglomerative) clustering methods.

In this study, the above clustering methods were examined with respect to their performance against three supervised similarity indices: 1) a peer-to-peer correlation metric (i.e., Jaccard coefficient), 2) an information theoretic-based approach (i.e., Normalized Mutual information (NMI)), and 3) a matching set similarity measurement index (accuracy).

The three supervised classifiers of multilayer perceptron (MLP), support vector machine (SVM), and k-nearest neighbor (kNN) were compared in terms of their ability to recognize three visually grouped species. In the back-propagation multilayer perceptron classifier, the number of neurons in the input layer was set equal to the number of features chosen while that of the output ones was set to 3 (equal to the three visually specified classes) with the logistic sigmoid functions used in the hidden layer. The MLP was trained using the Stochastic Gradient Descent (SGD) with the learning rate (η), the exponent for inverse scaling learning rate, and the momentum coefficient (μ) being set to 0.001, 0.5, and 0.6, respectively. Finally, the network was trained and tested for 1000 epochs. In addition, in the methodology proposed in this paper, the training datasets were classified using SVM with a Gaussian Radial Basis Function (RBF) kernel.

To develop classifiers, the dataset consisting of a total of 768 sliced blocks was randomly split into training and testing (at a split ratio of 80:20) datasets. Within the training set, the 10-fold cross-validation was employed to optimize the parameters and estimate the prediction performance of the models.

3. Results

3.1 Visually identified clusters

Despite a generally more or less similar sculpturing pattern, the seed characters of the selected *Vicia* species observed exhibited patterns of the papillose type projections (Figures 2-4), representing a variety of distinct shapes, heights, and coronations. The images taken from seed coat ornamentation did not show significantly adequate agreement with the classification proposed in Flora Iranica (Table 3).

Among the samples studied, the projections were either of a primary or a secondary type (only seen in *V. koeieana*). The primary ones could be described as tuberculate, colliculate, or aculeate. The proximal part of the projections showed a vertical profile of acute or obtuse retusus, truncate, or pungens but either curved or erect when seen from a lateral view. The tip of the projections in the images taken from above appeared rounded, elliptical, or satellite within the texture configuration. Based on the samples studied, three main projection type groups were recognized. The first group included seed coats in which the seed surface projections originated from the projection tips and continued to the background surface to form Colliculate or Tuberculate projections (Figure 2 a). This group included the species *V. koeieana*, *V. tetrasperma*, and *V. crocea*. Those seeds on which the projections originated from below the peak to form an Aculeate were in the second group, which included the species *V. angustifolia*, *V. villosa*, *V. pregrina*, *V. sativa*, *V. cappadocica*, *V. cinerea*, *V. ciceroidea*, *V. multijuga*, *V. akhmahgancia*, *V. aucheri*, *V. cracca*, and *V. ervilia* (Figures 2b & 3). Finally, the third group that contained the species *V. hyrcanica*, *V. variabilis*, and *V. michauxii* had projections starting from below the peak but formed Tuberculate projections (Figure 4). Figure 5 shows some of the salient seed coat topographic characters of the various species studied for use in developing the key.

A review of the literature reveals the rival theories on how to classify species into sections. For example, Boissier (Boissier and Buser 1888) divided the genus *Vicia* into two sects; namely, Sec. *Euvicia* and Sec. *Cracca* (as reported in Cronquist (Cronquist 1988)) while Engler (Engler 1892) divided it into the four Sec. *Euvicia*, Sec. *Cracca*, Sec. *Euvicia* (link) WDKOH, and Sec. *Euvicia* (L.) SF Grag. Other classifications have also been proposed (Fedchko 1948). No satisfactory agreement was observed between the images taken from seed coat ornamentation in this study and the four-way classification proposed in Flora Iranica; hence, the latter cannot be reliably used as a standard reference descriptor for the classification of *Vicia* species (Chrtková-Žertová 1979).

While most efforts on the classification of this genus have been based on such morphological characters as shape, size, and hilum location (Gunn 1971; Voronchikhin 1981), analysis of more species of the genus may reveal a greater variety in seed coats. This has been shown by Rashid *et al*. (Rashid et al. 2018) in their classification of the different species of the genus *Vicia* on the basis of seed characters. Extensive studies of morphological characters in other plants have been almost exhaustive, leaving out only a few characters and traits. However, the great differences and similarities among the plants in a species make their classification difficult. Indeed, a great many species do not lend themselves to individual study to the extent that most present-day scholars even claim that most observations in the past have been fallacious or misinterpreted. Consequently, much emphasis is being nowadays laid on trivial traits such as scale, hair, spores, or epidermal structure as descriptors for species or genus identification.

Pakravan *et al*. (Pakravan et al. 2001) showed that seed coat micro-ornamentation types are especially important as identifier characters, particularly in close species that have distinguishable differences such as pore-like structures on seed coat, albeit they are quite similar in a general way. The authors concluded that the ornamentation types could be used as distinguishing characters in very close species while judgment on more alien species had better be reduced to variety level.

It is, therefore, impossible to draw firm conclusions on the overall *Vicia* taxonomy based on the SEM analysis of only 18 species out of the 160 existing ones. Drawing upon previous work on the taxonomy of *Vicia* as a model and the results obtained from the present study, it might be suggested that seed coat ornamentation types (especially the size and shape of the projections on the seed external coat) might be regarded as the significant and systematic characters and that repeated images derived from image processing techniques might be exploited in novel classifications and interpretation of the results. In addition to identification for which these characters are primarily meant (e.g., recognition and pattern associations among individuals or groups as additional characteristics to distinguish different *Vicia* species), these characters could be utilized as the taxonomic key in plant sciences.

3.2 Clustering performance

Not all the proposed clustering approaches can generally yield satisfactory clustering results. Indeed, accuracy and Jaccard indices of less than 0.55 were recorded for all the clustering methods (Table 4). With all the conventional and deep feature sets, the visually classified species could not be reasonably discriminated; this was evidenced by accuracy values ranging from 0.36 to 0.55. While the mean-shift clustering method failed to recognize the visually identified clusters so that most of the CNNs feature sets were partitioned into less than three clusters, higher values of accuracy and Jaccard indices have been reported for this method. It might be Jaccard and Accuracy similarity indices provide incorrect information when the numbers of cluster members are dissimilar. NMI index fixes this problem by normalization. The results in the present case indicated that the three k-means, agglomerative, and Gaussian mixture clustering methods attained their highest NMI index values with the SFTA feature set (Table 4). Moreover, when these same clustering methods were used, the silhouette coefficient, which is an internal evaluation metric, was greater than 0.5 with all the feature spaces (Figure 6), confirming the existence of a clustering structure in the data.

Chuang *et al.* (Chuang et al. 2006) mentioned that image clustering with the use of spatial information such as image textural features mostly leads to undesirable results. Generally, common image clustering draws upon image segmentation based on pixel colors. Moreover, better clustering results can be achieved by combining color and texture features (Wei Tan et al. 2018). This is while SEM images are usually described as grayscale images and are colorless so that color features cannot be extracted.

Although the clustering based on SEM images was not successful in this study, it revealed the clustering structure inherent in the data. It also showed that SEM images of the same magnification and taken from a specified angle could surely improve the clustering performance since image resolution, magnification, and angle of view greatly affect clustering performance.

In conclusion, using a larger dataset with SEM images taken from a predefined direction and at known magnification ratios might be recommended if improved clustering performance and detection of the proposed method are sought.

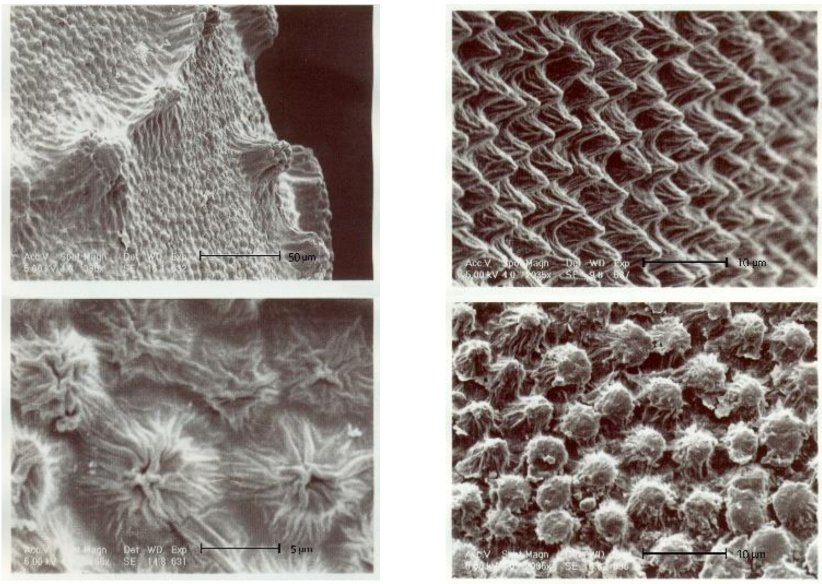

(a) (b)

Figure 2. a) A typical primary projection in *V. koeieana* seen as a Tuberculate type of the rounded or irregular shape on the seed, b) Primary projections in *V. ervilia* seen as Colliculate projections of the short type with elliptical to irregular forms (side- and front-view images are placed in the top and bottom rows, respectively).

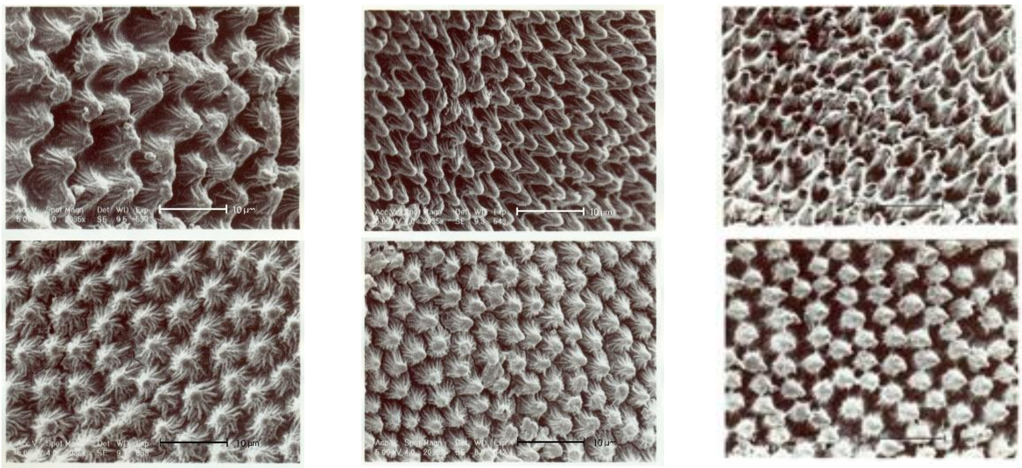

(a) (b) (c)

Figure 3. Primary projections in a) *V. akhmaghanica*, b) *V. craca*, and c) *V. peregrina*. The projections in all these species originate from below the peak to form an Aculeate and the proximal part of the projections exhibit a vertical profile of acute Aculeate (side- and front-view images are placed in the top and bottom rows, respectively).

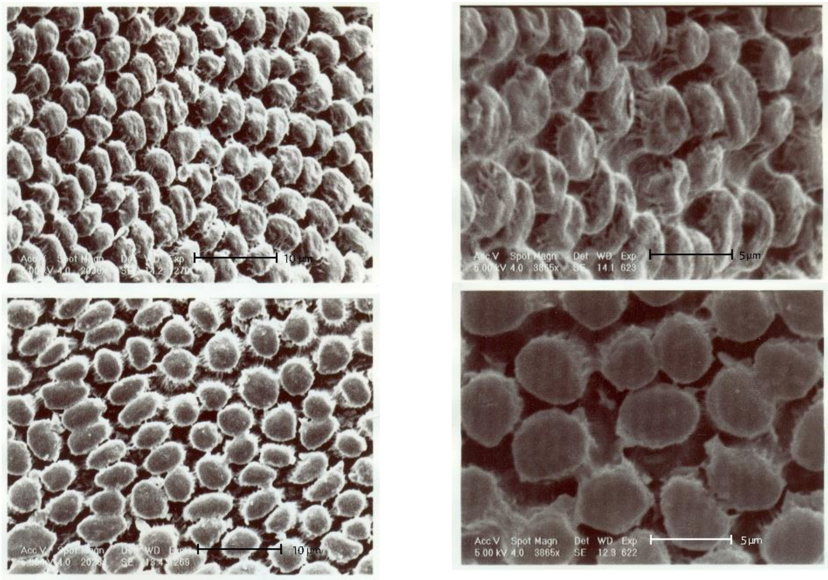

(a) **(b)**

Figure 4. Primary projections in a) *V. michauxii*, and b) *V. variabilis*. Features in the two species are seen as Tuberculate (side-view and front-view images are placed in the top and bottom rows, respectively).

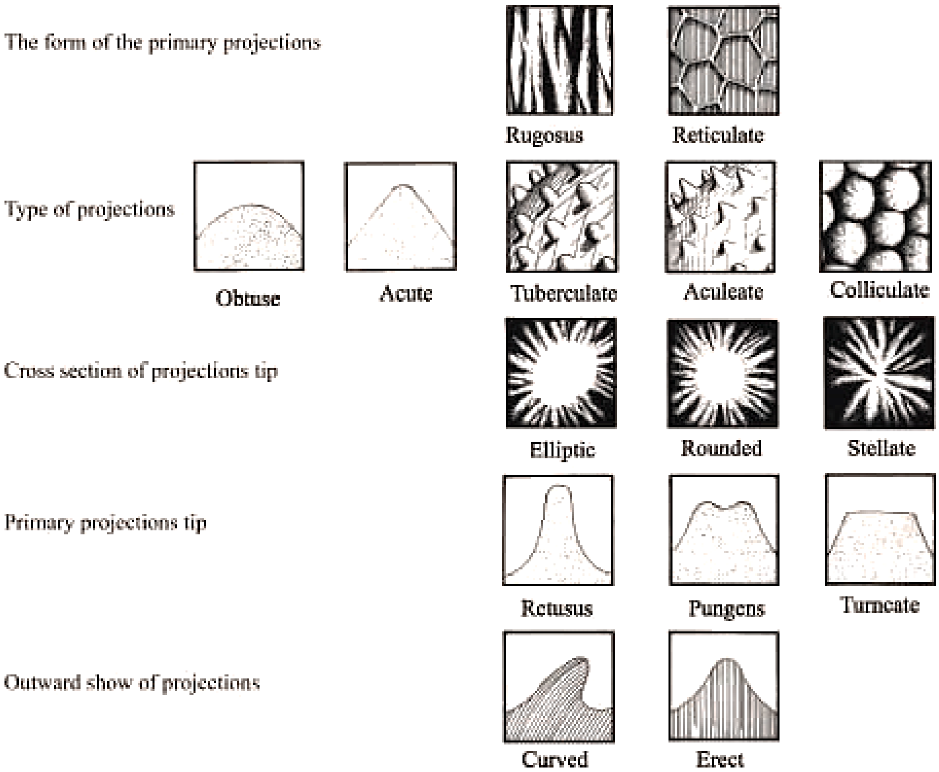

Figure 5. The description key for the seed coat ornamentation using Stern's terminology (Stern 1983).

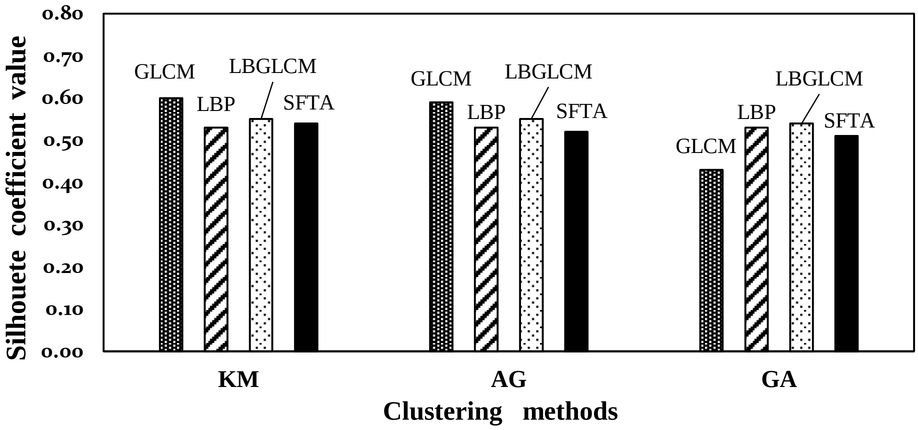

Figure 6. Computed Silhouette coefficient in evaluating the different clustering methods (KM: K-means, AG: Agglomerative, and GM: Gaussian Mixture).

Table 3. Seed micromorphological traits of eighteen *Vicia* species using SEM technology along with those of the species examined in different flora.

<table>
<tr><td>Main projection type group</td><td colspan="3">G1</td><td colspan="12">G2</td><td colspan="3">G3</td></tr>
<tr><td>Flora Orientalis</td><td></td><td></td><td colspan="4">Sect. II Cracca Series B</td><td></td><td></td><td></td><td></td><td></td><td>Sect. II. Cracca SeriesA</td><td colspan="3">Sect. I. Euvicia</td><td colspan="2">Sect. I. Euvicia</td><td></td></tr>
<tr><td>Flora of Turkey</td><td>Sect. Anatropostylia Plitm</td><td>Sect. Cracca S. F. Gray</td><td colspan="2">Sect. Ervum (L.) S. F. Gray</td><td colspan="2">Sect. Cracca S. F. Gray</td><td></td><td></td><td></td><td></td><td></td><td></td><td>Sect. Vicia</td><td colspan="2"></td><td colspan="2">Sect. Vicia</td><td></td></tr>
<tr><td>Selected Vicia species</td><td>1</td><td>2</td><td>3</td><td>4</td><td>5</td><td>15</td><td>6</td><td>7</td><td>8</td><td>9</td><td>10</td><td>11</td><td>12</td><td>13</td><td>14</td><td>16</td><td>17</td><td>18</td></tr>
<tr><td>Projection type</td><td>Ps</td><td colspan="2">Pt</td><td colspan="15">Pb</td></tr>
<tr><td>Seed surface pattern</td><td>T</td><td>T</td><td>C</td><td colspan="12">A</td><td colspan="3">T</td></tr>
<tr><td>Base and apex angles</td><td colspan="3">O</td><td colspan="15">Q</td></tr>
<tr><td>Seed shape</td><td colspan="11">Er</td><td colspan="6">Cu</td><td>Er</td></tr>
<tr><td>Characteristic projections at the tip of the seed</td><td colspan="3">S</td><td colspan="12">R</td><td colspan="3">El</td></tr>
</table>

Legend:

Ps: Primary and secondary projections Pt: Primary projections at the endmost tip (peak) Pb: Primary projections below the peak
T: Tuberculate A: Aculeate C: Colliculate
O: Obtuse Q: Acute
Cu: abaxially curved Er: abaxially erect

1. V. koeieana 2. *V. crocea* 3.*V. tetrasperma* 4. *V. ervilia* 5. *V. cappadocica* 6. *V. cinerea* 7. *V. cracca* 8. *V. akhmaghanica* 9. *V. aucherii*
10. V. multijuga 11. *V. ciceroideae* 12. *V. sativa* 13. *V. peregrina* 14. *V. angustifolia* 15. *V. villosa* 16. *V. michauxii* 17. *V. hyrcanica* 18. *V. variabilis*

Table 4. Clustering results with classical texture and CNN selected features when both side-view and front-view images were used.

		ACC	JAC	NMI			ACC	JAC	NMI
GLCM	KM	0.39	0.24	0.02	ResNet50	KM	0.54	0.37	0.10
	AG	0.45	0.29	0.02		AG	0.42	0.26	0.10
	GM	0.38	0.23	0.02		GM	0.42	0.26	0.10
	MS	0.39	0.24	0.02		MS	0.5*	0.33*	0.00*
LBP	KM	0.41	0.26	0.03	VGG16	KM	0.42	0.26	0.07
	AG	0.37	0.23	0.01		AG	0.50	0.33	0.05
	GM	0.39	0.24	0.02		GM	0.37	0.25	0.05
	MS	0.4	0.25	0.02		MS	0.5*	0.33*	0.00*
LBGLCM	KM	0.47	0.31	0.06	VGG19	KM	0.42	0.27	0.08
	AG	0.44	0.28	0.05		AG	0.5	0.33	0.05
	GM	0.38	0.23	0.09		GM	0.36	0.19	0.06
	MS	0.38	0.23	0.06		MS	0.50*	0.33*	0.00*
SFTA	KM	0.44	0.28	0.15	Xception	KM	0.33	0.2	0.07
	AG	**0.50**	**0.33**	**0.16**		AG	**0.55**	**0.37**	**0.14**
	GM	0.48	0.32	0.12		GM	0.40	0.26	0.09
	MS	0.47	0.31	0.08		MS	0.44	0.29	0.1

KM: K-means, AG: Agglomerative, GM: Gaussian Mixture, MS: Mean-shift
ACC: Accuracy index, JAC: Jaccard index, NMI: Normalized Mutual Information index.
* Mean-shift clustering method failed to recognize the visually identified clusters, feature sets were partitioned into less than three clusters.

3.3 Classification Results

Based on the classification performances reported in Table 5, the best results were recorded for SFTA feature space. When both side-view and front-view images were used for the classification, a MLP with two hidden layers of 10 and 5 neurons achieved the best accuracy values of 90% and 85% in the training and testing processes, respectively. However, classification accuracy rose just when side-view images were used. In this case, a MLP with two hidden layers of 6 and 3 neurons achieved its best accuracy values of 96% and 88% in the training and testing sets, respectively. Results also revealed that the accuracy index values of SVM and kNN were not significantly different from those obtained with MLP.

The classification performances of different deep feature extraction models are summarized in Table 5. Clearly, three classes were better separated in the deep feature sets than they were in the conventional ones. Xception yielded the best classification result. As reported in Table 5, the deep feature extraction methods outperformed the SFTA traditional textural descriptors. The features yielded by Xception and a neural network with two hidden layers of 10 and 5 neurons led to better classification results with the high accuracy values of 99% and 96% in the training and testing sets, respectively. In agreement with these results, Wei Tan *et al.* (Wei Tan et al. 2018) reported that the best method for the classification of plant species would be a MLP classifier with CNN features. Similar studies conducted on texture analysis of SEM images not only indicated the effectiveness of combining deep and textural features (Cai et al. 2022) but also showed that convolutional neural networks would perform equally well or better than the traditional algorithms (Liu L et al. 2016; Liu X and Aldrich 2022). The high capability of pre-trained neural networks has also been demonstrated in barley varietal classification with an accuracy value of less than 75% in varietal classification when color, texture, and morphological attributes were used and above 93% when pre-trained convolutional neural networks were employed (Kozłowski et al. 2019).

Table 5. Classification results with classical texture and CNNs selected features when both side-view and front-view images were used.

		Accuracy index				Accuracy index	
		Train	Test			Train	Test
GLCM	MLP	0.66	0.65	ResNet50	MLP	0.96	0.74
	SVM	0.65	0.63		SVM	0.97	0.73
	KNN	0.75	0.54		KNN	0.84	0.71
LBP	MLP	0.74	0.70	VGG16	MLP	0.99	0.75
	SVM	0.72	0.70		SVM	0.97	0.72
	KNN	0.81	0.62		KNN	0.86	0.70
LBGLCM	MLP	0.71	0.67	VGG19	MLP	0.96	0.75
	SVM	0.71	0.66		SVM	0.96	0.71
	KNN	0.81	0.57		KNN	0.84	0.75
SFTA	MLP	**0.90**	**0.85**	Xception	MLP	**0.99**	**0.96**
	SVM	0.88	0.80		SVM	0.99	0.94
	KNN	0.91	0.81		KNN	0.98	0.94

MLP: Multilayer perceptron, SVM: Support Vector Machine, KNN: K-Nearest Neighbors.

Regarding the application of pre-trained CNN models coupled with common classifiers, the results obtained proved consistent with those used VGG16+SVM in the determination of physiological disorders in apple (Buyukarikan and Ulker 2022), DenseNet169+MLP model in classifying rice plant diseases (Narmadha et al. 2022), AlexNet + SVM in assessing the severity of tomato late blight disease (Verma et al. 2020), and classifying rice plant disease (Shrivastava et al. 2019) where reached the highest accuracy of 96.11, 97.68%, 93.4% and 91.37%, respectively.

In conclusion, the deep models were found capable of extracting effective features for classification equally well or even better than the conventional image texture analysis methods despite the fact that they had not been trained using colorless SEM images of seed coat surfaces.

4. Conclusion

The paper reported on the significance of SEM image observations and analysis for the classification of the different species of the genus *Vicia* into different sections. In agreement with recent studies (Asadova and Asgarov 2018), the study showed that the diversity in seed coat ornamentation is far less flexible and variable compared to that in growth and flowering structures and that seed coat ornamentation could, thus, be exploited to disclose interspecies diversity. The visual classification developed in this study showed that micromorphological traits could be used as good distinctive criteria. Image analysis of *Vicia* species coupled with clustering and the classification of this genus based on morphological characters (microtaxonomy) could efficiently differentiate the *Vicia* species. All the pre-trained CNNs deep feature extractors were found to perform equally well or better than the traditional algorithms (GLCM, LBP, LBGLCM, and SFTA). Of the four CNNs used in this study, Xception yielded the most reliable features and the best classification results were obtained using a MLP classifier. Transfer learning was exploited to reduce the labor-intensive aspects of the taxonomic classification of the genus based on seed coat surfaces. However, the scientific impact of this research should be augmented by studying more samples to develop a more accurate and robust classifier.

Acknowledgment

The authors would like to express their gratitude to the Deputy for Research, Isfahan University of Technology, for the financial support granted.

References

1. Aedo, C. 2016. Taxonomic Revision of Geranium sect. Polyantha (Geraniaceae) 1. Ann. Missouri Bot. Gard., 101(4):611-635.
2. Ariunzaya, G., Kavalan, J. C. and Chung, S. 2023. Identification of seed coat sculptures using deep learning. J. Asia-Pac. Biodivers., 16(2):234-245.
3. Asadova, K. and Asgarov, A. 2018. Distribution and Ecobiological Research of Vetch (Vicia L.) Species in Azerbaijan. Int. J. Curr. Res. Biosci. Plant Biol., 5(7):27-36.
4. Boissier, E. and Buser, R. 1888. Flora orientalis; sive, Enumeratio plantarum in oriente a Graecia et Aegypto ad Indiae fines hucusque observatarum: Supplementum editore R. Buser. apud H. Georg.

5. Buyukarikan, B. and Ulker, E. 2022. Classification of physiological disorders in apples fruit using a hybrid model based on convolutional neural network and machine learning methods. Neural Comput. Appl. 34(19):16973-16988.
6. Cai, J., Liu, M., Zhang, Q., Shao, Z., Zhou, J., Guo, Y., Liu, J., Wang, X., Zhang, B. and Li, X. 2022. Renal cancer detection: fusing deep and texture features from histopathology images. Biomed Res. Int. 2022.
7. Chrtková-Žertová, A. 1979. Vicia. Flora Iranica. 140:16-56.
8. Chuang, K. S., Tzeng, H. L., Chen, S., Wu, J. and Chen, T. J. 2006. Fuzzy c-means clustering with spatial information for image segmentation. Comput. Med. Imaging Graph. 30(1):9-15.
9. Cronquist, A. 1988. The evolution and classification of flowering plants. New York Botanical Garden.
10. Engler, A. 1892. Syllabus der pflanzenfamilien. Vol. 2. Gebrüder Borntraeger Verlag.
11. Fedchko, B. A. 1948. Flora of the USSR (Flora SSSR). Vol. 13. Koeltz Scientific Books, Koenigsteine.
12. Gabr, D. G. 2018. Significance of fruit and seed coat morphology in taxonomy and identification for some species of Brassicaceae. Am. J. Plant Sci., 9(03):380.
13. Genze, N., Bharti, R., Grieb, M., Schultheiss, S. J. and Grimm, D. G. 2020. Accurate machine learning-based germination detection, prediction and quality assessment of three grain crops. Plant methods, 16(1):1-11.
14. Gunn, C. R. 1971. Seeds of native and naturalized vetches of North America. US Agricultural Research Service, 392.
15. Ilakiya, J. and Ramamoorthy, D. 2021. SEM and light microscopic studies in seeds of Hibiscus surattensis L. and phylogenetic attributes in Puducherry region, India. Geol. Ecol. Landsc. 5(4):269-279.
16. Jalal, M., Shaheen, S., Saddiqe, Z., Harun, N., Abbas, M. and Khan, F. 2021. Scanning electron microscopic screening; Can it be a taxonomic tool for identification of traditional therapeutic plants. Microsc. Res. Tech. 84(4):730-745.
17. Kaus, M. R., Warfield, S. K., Nabavi, A., Black, P. M., Jolesz, F. A. and Kikinis, R. 2001. Automated segmentation of MR images of brain tumors. Radiology, 218(2):586-591.
18. Kozłowski, M., Górecki, P. and Szczypiński, P. M. 2019. Varietal classification of barley by convolutional neural networks. Biosyst. Eng. 184:155-165.

19. Liu, L., Fieguth, P., Wang, X., Pietikainen, M. and Hu, D. 2016. Evaluation of LBP and deep texture descriptors with a new robustness benchmark. Computer Vision–ECCV: 14th European Conference, Amsterdam, The Netherlands, October 11-14, 2016, Springer.
20. Liu, X. and Aldrich, C. 2022. Deep learning approaches to image texture analysis in material processing. Metals, 12(2):355.
21. Luo, T., Zhao, J., Gu, Y., Zhang, S., Qiao, X., Tian, W. and Han, Y. 2021. Classification of weed seeds based on visual images and deep learning. Inf, Process. Agric., 10(1): 40-51.
22. Narmadha, R., Sengottaiyan, N. and Kavitha, R. 2022. Deep transfer learning based rice plant disease detection model. Intell. Autom. Soft Comput. 31(2): 1257-1271.
23. Pakravan, M., Hayel Moghaddam, K. and Ghahreman, A. 2001. Use of micromorphological data for classification in the genus Alcea (Malvaceae). In Proceeding of deep morphology; 18-21 October; University of Vienna, Austria.
24. Pieniazek, F. and Messina, V. 2016. Scanning electron microscopy combined with image processing technique: Microstructure and texture analysis of legumes and vegetables for instant meal. Microsc. Res. Tech., 79(4):267-275.
25. Prasad, R., Mukherjee, K. and Gangopadhyay, G. 2014. Image-analysis based on seed phenomics in sesame. Plant Breed. Seed Sci. 68(1):119.
26. Przybyło, J. and Jabłoński, M. 2019. Using Deep Convolutional Neural Network for oak acorn viability recognition based on color images of their sections. Comput. Electron. Agric. 156:490-499.
27. Rashid, N., Zafar, M., Ahmad, M., Malik, K., Haq, I., Shah, S. N., Mateen, A. and Ahmed, T. 2018. Intraspecific variation in seed morphology of tribe vicieae (Papilionoidae) using scanning electron microscopy techniques. Microsc. Res. Tech. 81(3):298-307.
28. Rashid, N., Zafar, M., Ahmad, M., Memon, R. A., Akhter, M. S., Malik, K., Malik, N. Z., Sultana, S. and Shah, S. N. 2021. Seed morphology: An addition to the taxonomy of Astragaleae and Trifolieae (Leguminosae: Papilionoidae) from Pakistan. Microsc. Res. Tech., 84(5):1053-1062.
29. Ribas, L. C., Junior, J. J. dM. S, Scabini, L. F. and Bruno, O. M. 2020. Fusion of complex networks and randomized neural networks for texture analysis. Pattern Recognit., 103:107189.
30. Shrivastava, V. K., Pradhan, M. K., Minz, S. and Thakur, M. P. 2019. Rice plant disease classification using transfer learning of deep convolution neural network. Int. Arch. Photogramm. Remote Sens. Spat. Inf. Sci., 42:631-635.
31. Stern, W. T. 1983. Botanical Latin. 3 ed. London: Thomas Nelson.

32. Szkudlarz, P. and Celka, Z. 2016. Morphological characters of the seed coat in selected species of the genus Hypericum L. and their taxonomic value. Biodivers. Res. Conserv., 44(1):1-9.

33. Taheri-Garavand, A., Nasiri, A., Fanourakis, D., Fatahi, S., Omid, M. and Nikoloudakis, N. 2021. Automated in situ seed variety identification via deep learning: a case study in chickpea. Plants, 10(7):1406.

34. Verma, S., Chug, A. and Singh, A. P. 2020. Application of convolutional neural networks for evaluation of disease severity in tomato plant. J. Discret. Math. Sci. Cryptogr. 23(1):273-282.

35. Voronchikhin, V. 1981. Identification of certain species of the genus Vicia L. from their fruits and seeds.

36. Wei Tan, J., Chang, S. W., Abdul-Kareem, S., Yap, H. J. and Yong, K. T. 2018. Deep learning for plant species classification using leaf vein morphometric. IEEE/ACM Trans. Comput. Biol. Bioinform., 17(1):82-90.

37. Yang, S., Zheng, L., He, P., Wu, T., Sun, S. and Wang, M. 2021. High-throughput soybean seeds phenotyping with convolutional neural networks and transfer learning. Plant Methods, 17(1):50.

طبقه بندی برخی از گونه های *Vicia* ایرانی با استفاده از تحلیل و تفسیر بافت تصاویر SEM به روش مرسوم و یادگیری عمیق

مهرنوش جعفری، سید علی محمد میرمحمدی میبدی، و محمد حسین اهتمام

چکیده

ویژگی‌های میکرومورفولوژیکی برجستگی‌های روی سطح دانه ممکن است در شناسایی گونه‌های جنس *Vicia* مؤثر باشند. مطالعه حاضر به منظور تعیین اینکه آیا داده‌های ریزساختاری و تزئینات پوشش دانه به‌دست‌آمده از تصاویر SEM می‌توانند به عنوان ابزار کافی برای شناسایی جنس *Vicia* استفاده شوند، انجام شد. به غیر از بررسی بصری، انواع روش های مبتنی بر بافت، از جمله چهار روش مرسوم GLCM، LBP، LBGLCM، و SFTA، و چهار شبکه عصبی کانولوشن از پیش آموزش دیده (یعنی ResNet50، VGG16، VGG19، و Xception) برای استخراج ویژگی ها و دسته بندی گونه های جنس *Vicia* با استفاده از تصاویر SEM استفاده شد. در مرحله بعدی، چهار روش طبقه‌بندی k-means، Meanshift، agglomerative و Gaussian mixture بدون نظارت برای گروه‌بندی گونه‌های Vicia شناسایی‌شده بر اساس ویژگی‌های استخراج‌شده، مورد بهره‌برداری قرار گرفتند. همچنین، سه طبقه‌بندی‌کننده با نظارت شامل شبکه پرسپترون چندلایه (MLP)، ماشین بردار پشتیبان (SVM) و k-نزدیک‌ترین همسایه (kNN) از نظر قابلیت در تمایز دسته‌های مختلف شناسایی‌شده به روش بصری، مقایسه شدند. نتایج SEM نشان داد که ممکن است سه کلاس بر اساس پیوندهای ریزمورفولوژیکی صفت-گونه شناسایی شود و تفاوت بین گونه‌ها در جنس *Vicia* و اعتبار *Vicia sativa* قابل تأیید است. با توجه به نتایج طبقه‌بندی‌کننده‌ها، عملکرد توصیفگر بافتی SFTA از الگوریتم‌های GLCM، LBP و LBGLCM بهتر بود اما عملکرد ضعیف‌تری نسبت به مدل‌های یادگیری عمیق، نشان داد. مدل ترکیبی Xception و MLP در تفکیک گونه‌ها در جنس *Vicia* با بهترین عملکرد طبقه‌بندی به ترتیب 99٪ و 96٪ در آموزش و آزمون موفق بود.